PHYSICAL REVIEW B **74**, 085321 (2006)

Electron-phonon scattering at the intersection of two Landau levels

V. N. Golovach*
School of Physics, University of Exeter, Stocker Road, Exeter EX4 4QL, United Kingdom

M. E. Portnoi†
International Center for Condensed Matter Physics, Universidade de Brasília, 70919-970 Brasília-DF, Brazil and School of Physics, University of Exeter, Stocker Road, Exeter EX4 4QL, United Kingdom

(Received 1 March 2006; revised manuscript received 19 July 2006; published 29 August 2006)

We predict a double-resonant feature in the magnetic field dependence of the phonon-mediated longitudinal conductivity σ_{xx} of a two-subband quasi-two-dimensional electron system in a quantizing magnetic field. The two sharp peaks in σ_{xx} appear when the energy separation between two Landau levels belonging to different size-quantization subbands is favorable for acoustic-phonon transitions. One-phonon and two-phonon mechanisms of electron conductivity are calculated and compared. The phonon-mediated interaction between the intersecting Landau levels is considered and no avoided crossing is found at thermal equilibrium.

DOI: 10.1103/PhysRevB.74.085321 PACS number(s): 73.63.Hs, 73.43.Qt, 73.40.Kp, 63.20.Kr

I. INTRODUCTION

The acoustic phonon scattering of electrons in two-dimensional (2D) systems in quantizing magnetic fields has been studied extensively over the last three decades. The peculiar density of states of the 2D electrons in a transverse magnetic field **B** results in suppression of the electron-phonon stattering rate at strong magnetic fields,[1,2] at which the so-called *inelasticity* parameter $\eta=s/\lambda\omega_c$ is less than unity, where s is the sound velocity, $\lambda=\sqrt{\hbar/eB}$ is the magnetic length, and $\omega_c=eB/m$ is the cyclotron frequency. A detailed analysis of the acoustic phonon emission and absorption spectra in 2D electron systems has been carried out in connection with phonon absorption spectroscopy,[3–6] which is used to investigate electronic states in both integer and fractional quantum Hall effects. It was also noticed that at a certain stage of supression of the one-phonon inter-Landau-level transitions, the two-phonon transitions dominate the electron relaxation rate.[8] However, in a two-subband system the electron relaxation rate can still be due to the one-phonon transitions occurring between Landau levels of different size-quantization subbands. An oscillatory behavior of the electron lifetime was found in a two-subband system.[9]

In this paper we focus on an intersection of two Landau levels belonging to different size-quantization subbands of a two-dimensional electron gas in a transverse magnetic field **B** (see Fig. 1). The electron density is chosen so that there are enough electrons to fill only one Landau level out of the two at the intersection point. Despite the general suppression due to small η, we find that at an energy separation between the two Landau levels of the order of the characteristic acoustic-phonon energy $T_\lambda=\hbar s/\lambda$, the electron-phonon scattering is strongly enhanced. In what follows we neglect the effects related to the Coulomb interaction between the electrons. These effects significantly change the results at low temperatures.[10,11] The virtue of the considered structure, from the point of view of electron-phonon scattering, is that an enhancement of the dissipative conductivity σ_{xx} arises against the background of its strong overall suppression. This enhancement can be understood from the following physical consideration.

At the intersection of two Landau levels, say level $\ell=0$ of the upper subband and level $\ell=1$ of the lower subband, the matrix element of the electron-phonon interaction requires a phonon momentum $q\sim 1/\lambda$ for the most efficient transition. Note that two Landau levels can cross at a magnitude of **B** corresponding to $\lambda\sim a$, where a is the characteristic width of the quantum well confining the two-dimensional electron gas. This results in $q_z\sim q_\perp\sim 1/\lambda$, where q_z and $q_\perp$ are the perpendicular and in-plane components of the phonon momentum, respectively. On the other hand, the energy conservation law requires that the phonon energy $\hbar\omega_{\mathbf{q}}$ matches the energy separation between the two Landau levels, $\Omega=|\mathcal{E}_{\ell=0}-\mathcal{E}_{\ell=1}|$. For acoustic phonons we have $\omega_{\mathbf{q}}=sq$, and if combined with the momentum requirement, two *resonances* are obtained, one on each side of the crossing point, corresponding to $\Omega\simeq\hbar s/\lambda\equiv T_\lambda$. At each resonance the electron-phonon scattering is significantly enhanced, owing to the one-phonon transitions.

It is worth noting that a simultaneous intersection of two Landau levels with the Fermi level leads to a missing quantum Hall effect plateau, as expected from a single-subband consideration. Such intersections occur repeatedly with decreasing B if the electron density per spin orientation n_{2D}

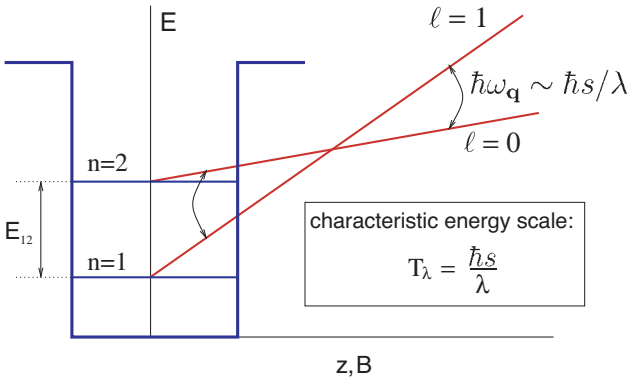

FIG. 1. (Color online) A crossing of two Landau levels belonging to different subbands of size quantization. Phonon transitions are most favorable for phonons with $q\sim 1/\lambda$.

$=n_c[1+(2p-1)/q]$, where p and q are positive integers, and $n_c=mE_{12}/2\pi\hbar^2$, with E_{12} being the energy separation between the two size-quantization subbands. However, if the Coulomb interaction between the electrons is taken into account, a *new* energy gap emerges at the intersection point.[10]

An enhancement of the electron scattering in a two-subband system occurs also at zero magnetic field, when the second size-quantization subband starts being filled with electrons. This effect can be viewed in terms of a Lifshitz topological transition of the Fermi surface, which is well-known for the 3D case.[12] The 2D case of this transition was considered in Ref. 13, where the electron scattering occured on a random potential of impurities. At $B\neq 0$ one can hardly speak of a Fermi surface. However, we refer the peculiar behavior of σ_{xx} in our case to the same origin—a strong variation in the density of states at the Fermi level. The case considered in this paper has the advantage of more pronounced anomalies.

An experimental realization of the above-described situation can be acheived in GaAs/AlGaAs heterojunctions. Usually, the donor supply of the electrons into the 2D layer is not sufficient to achieve filling of the second size-quantization subband. However, a significant increase in the concentration can be achieved by illuminating the sample with photons of energy close to the band gap of GaAs. The photoexcited electrons come either from the DX centers in the AlGaAs layer[14] or from the valence band of the bulk GaAs producing a charge separation at the interface.[15] Furthermore, the 2D electron concentration can be tuned within a large range using the method of continuous photoexcitation.[16] Population of the second subband of size quantization in a magnetic field has been observed in a number of experiments related to magneto-optical studies of the integer and fractional quantum Hall effects.[17–19]

In this paper we consider only scattering of electrons by phonons, although in a real 2D system the main contribution to σ_{xx} at low temperatures comes from the scattering of electrons by the impurity potential. This has been studied extensively in connection with the integer quantum Hall effect. However, since the electron-phonon coupling constant $\alpha \sim B$, the phonon-induced σ_{xx} at high enough magnetic fields may be comparable with the impurity-induced σ_{xx}.

II. GENERAL RELATIONS

We consider an electron gas in a quantum well, formed by a confining potential $V(z)$, in a strong magnetic field $\mathbf{B}$ directed along the z axis. In the Landau gauge the vector potential $\mathbf{A}=(0,xB,0)$, and the electron can be characterized by the center of orbit coordinate X. The energy spectrum of the electron, $\mathcal{E}_{n\ell}=E_n+\hbar\omega_c(\ell+1/2)$, consists of the size quantization energy E_n and the magnetic quantization energy, described by the Landau level number ℓ. The acoustic phonons, with dispersion $\omega_{\mathbf{q}j}$, interact with the electrons via both deformation potential (DP) and piezoelectric (PE) mechanisms. We shall restrict ourselves to the isotropic Debye approximation, in which the phonon modes fall into a branch of longitudinal (LA) phonons ($j=1$) and two branches of transverse (TA) phonons ($j=2,3$). This seems to be a good approximation for phonons at thermal equilibrium, in contrast with the case of ballistic phonon propagation, where the anisotropy gives rise to self-focusing effects.[21] For GaAs, it follows that the DP mechanism couples electrons only with LA phonons. We assume that acoustic phonons are the only sourse of scattering for the electrons in the well, neglecting the effects of interface roughness and random potential of impurities, as well as the presence of optical phonon modes. This assumption is valid for fairly pure samples at temperatures below the optical phonon energy. We also suppose the acoustical phonons to be three-dimensional, neglecting the effects of interface phonons. The electrons are considered spinless. The spin degeneracy can be easily accounted for at the final stage of calculation. Electron scattering by phonons is spin-preserving, and the results for the conductivity will differ only by a factor of 2.

The system of interacting electron and phonon gases is described by the following second quantized Hamiltonian:

$$H=H_0+H_{int}, \tag{1}$$

with

$$H_0=\sum_{n\ell X}\mathcal{E}_{n\ell}C^\dagger_{n\ell X}C_{n\ell X}+\sum_{\mathbf{q}j}\hbar\omega_{\mathbf{q}j}(b^\dagger_{\mathbf{q}j}b_{\mathbf{q}j}+1/2), \tag{2}$$

and

$$H_{int}=-\sum_{\substack{n\ell n'\ell'\\ \mathbf{q}jX}}M^{\mathbf{q}j}_X\begin{pmatrix}n'\ell'\\ n\ell\end{pmatrix}(b^\dagger_{-\mathbf{q}j}+b_{\mathbf{q}j})C^\dagger_{n'\ell' X-\lambda^2 q_y}C_{n\ell X}. \tag{3}$$

Here $C^\dagger_{n\ell X}$, $C_{n\ell X}$, and $b^\dagger_{\mathbf{q}j}$, $b_{\mathbf{q}j}$ stand for the creation and annihilation operators of the electron and phonon, respectively. The matrix element of electron-phonon interaction is given by

$$M^{\mathbf{q}j}_X\begin{pmatrix}n'\ell'\\ n\ell\end{pmatrix}=(e\beta_{\mathbf{q}j}-iq\Xi_{\mathbf{q}j})\sqrt{\frac{\hbar}{2\omega_{\mathbf{q}j}\rho_c V_{3d}}}\times F_{nn'}(q_z)\Omega_{\ell\ell'}(q_\perp)e^{iq_x(X-\lambda^2q_y/2)+i\varphi(\ell-\ell')}, \tag{4}$$

where $q_\perp=\sqrt{q_x^2+q_y^2}$ is the value of the in-plane component of the phonon wave vector $\mathbf{q}$, and φ is the polar angle of $\mathbf{q}_\perp$, counted from the x axis. The sample volume and density are noted by V_{3d} and ρ_c, respectively. The factor $\Omega_{\ell\ell'}(q_\perp)$ for $\ell\geqslant\ell'$ reads

$$\Omega_{\ell\ell'}(q_\perp)=i^{\ell-\ell'}\left(\frac{\ell'!}{\ell!}\right)^{1/2}e^{-\chi^2/2}\chi^{\ell-\ell'}L^{\ell-\ell'}_{\ell'}(\chi^2), \tag{5}$$

where $\chi^2=\lambda^2q_\perp^2/2$ and $L^m_n(x)$ are the associated Laguerre polynomials. For $\ell<\ell'$, $\Omega_{\ell\ell'}(q_\perp)$ is obtained from Eq. (5) by interchanging the indices ℓ and ℓ' in the right-hand side of Eq. (5). The parameter $\Xi_{\mathbf{q}j}$ is introduced as follows:

$$\Xi_{\mathbf{q}j} = \frac{1}{2q}\Xi^{\mu\nu}[q_\mu e_\nu^{(j)}(\mathbf{q}) + q_\nu e_\mu^{(j)}(\mathbf{q})], \tag{6}$$

where $\Xi^{\mu\nu}$ is the deformation potential tensor and $\mathbf{e}^{(j)}(\mathbf{q})$ is the polarization vector of the jth phonon branch. For GaAs it reduces to $\Xi_{\mathbf{q}j}=\Xi_0\delta_{j1}$, with $\Xi_0\sim 7$ eV. The parameter $\beta_{\mathbf{q}j}$ is introduced as follows:

$$\beta_{\mathbf{q}j} = \frac{4\pi}{2q^2\kappa}\beta^{\mu\nu\omega}q_\mu[q_\nu e_\omega^{(j)}(\mathbf{q}) + q_\omega e_\nu^{(j)}(\mathbf{q})], \tag{7}$$

where $\beta^{\mu\nu\omega}$ is the piezomodulus tensor and κ is the relative permittivity of the material. In GaAs the piezomodulus tensor is completely symmetric and only one of its off-diagonal components is nonzero. The value of this component is denoted by h_{14} and is approximately 0.14 $\mathrm{C/m^2}$ in GaAs. The parameter $\beta_{\mathbf{q}j}$ thus depends only on the spatial orientation of the vector $\mathbf{q}$ and can be presented in the following form:

$$\beta_{\mathbf{q}1} = \beta_0\frac{3}{2}\sin^2\theta\cos\theta\sin 2\varphi,$$

$$\beta_{\mathbf{q}2} = \beta_0\frac{1}{2}\sin 2\theta\cos 2\varphi,$$

$$\beta_{\mathbf{q}3} = \beta_0\frac{1}{2}(3\cos^2\theta - 1)\sin\theta\sin 2\varphi, \tag{8}$$

where $\beta_0=(4\pi/\kappa)h_{14}$, and θ is the angle between $\mathbf{q}$ and the z axis. The quantum well form factor $F_{nn'}(q_z)$ is defined as

$$F_{nn'}(q_z) = \int \psi_{n'}(z)e^{iq_z z}\psi_n(z)dz, \tag{9}$$

where $\psi_n(z)$ is the nth size quantization level wave function (chosen to be real), which is completely determined by the confining potential $V(z)$. As a general feature, the factor $F_{nn'}(z)=\delta_{nn'}$ at $q_z \ll 1/a$ is of the order of unity at $q_z\sim 1/a$, and rapidly tends to zero at $q_z \gg 1/a$, where a is the characteristic size measure entering $V(z)$.

The matrix element (4) possesses the following symmetry relation:

$$M_X^{\mathbf{q}j}\begin{pmatrix} n'\ell' \\ n\ell \end{pmatrix} = \left[M_{X-\lambda^2 q_y}^{-\mathbf{q}j}\begin{pmatrix} n\ell \\ n'\ell' \end{pmatrix}\right]^*. \tag{10}$$

We calculate σ_{xx} starting from Kubo's formula for the conductivity tensor[22]

$$\sigma_{\mu\nu}(\omega) = \frac{1}{V_{2d}}\int_0^\infty dt e^{-i\omega t}\int_0^\beta d\lambda\langle J_\nu(-i\hbar\lambda)J_\mu(t)\rangle, \tag{11}$$

which gives the exact amplitude and phase of the induced current in an applied electric field of frequency ω. Here, $\mathbf{J}(t)$ is the current operator in the Heisenberg representation, V_{2d} is the area of the 2D plane, and $\beta=1/T$, where T is the temperature measured in energy units. The average denoted by the angle brackets in Eq. (11) is carried out in the grand canonical ensemble with the density matrix

$$\rho = \frac{1}{Z}\exp\{-\beta(H-\mu N)\}, \tag{12}$$

where μ is the electron chemical potential, N is the electron number operator, and Z is the partition function of the system of electrons and phonons.

In the case of a quantizing magnetic field, the events of electron scattering are rare if compared to the frequency of the orbital motion (cyclotron frequency). One can say that the electron orbital degree of freedom is frozen, and the electron scattering occurs between states characterized by the center of orbit coordinates X and Y.[23] The electron conductivity can then be related to the migration of the electron center of orbit.[24,25] Mathematically, it involves replacing the current operator $\mathbf{J}$ in Eq. (11) by $-e\dot{\mathbf{R}}$, where $\mathbf{R}\equiv(X,Y)$ is the radius vector of the electron center of orbit, and adding an antisymmetric tensor with xy-component $-en_{2D}/B$ to the conductivity tensor, where n_{2D} is the 2D electron density. The coordinates X and Y cannot be measured simultaneously. Their operators satisfy the commutation relation $[X,Y]=i\lambda^2$. The operator $\mathbf{R}$ satisfies the following equation of motion:

$$\dot{\mathbf{R}} = \frac{i}{\hbar}[H_{int},\mathbf{R}]. \tag{13}$$

We shall restrict ourselves to the study of the dissipative conductivity alone. For this purpose we rewrite the xx-component of Eq. (11) in an equivalent form:

$$\sigma_{xx} = \lim_{\delta\to+0}\frac{1}{i\omega+\delta}\left[\phi_{xx}(0) + \int_0^\infty e^{-i\omega t-\delta t}\dot{\phi}_{xx}(t)dt\right], \tag{14}$$

where the response function $\phi_{xx}(t)$ is given by

$$\phi_{xx}(t) = e^2\int_0^\beta \langle\dot{X}(-i\hbar\lambda)\dot{X}(t)\rangle d\lambda, \tag{15}$$

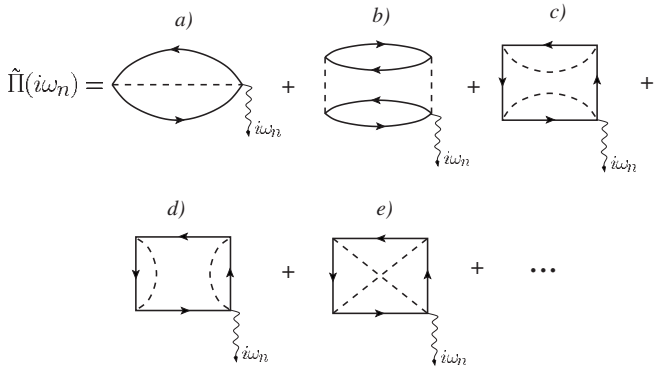

FIG. 2. S-matrix expansion of the two-particle Green's function $\Pi(\tau)$. The solid line and the dashed line represent the Green's functions of the unperturbed electron and phonon, respectively. The wavy line is introduced to account for the Matsubara frequency $i\omega_n$ and for the action of the operator $\hat{Q}_y$.

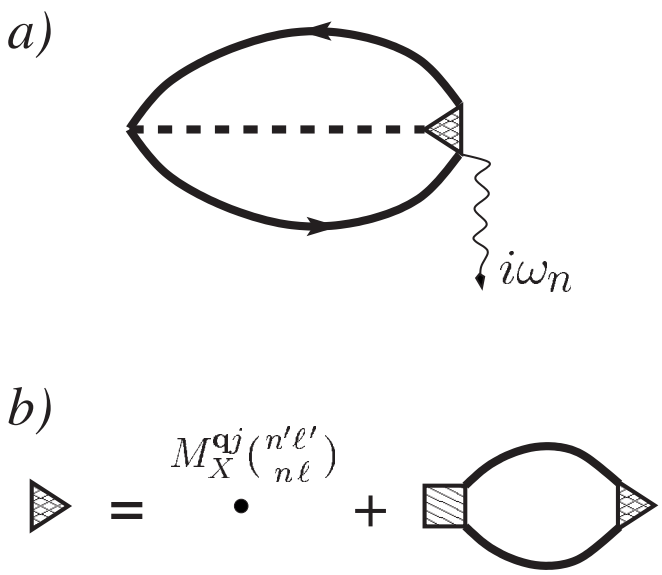

FIG. 3. Results of graphical summation of the perturbation series expansion. (a) A diagram for the exact $\tilde{\Pi}(i\omega_n)$ expressed in terms of the exact electron Green's function (solid line), the exact phonon Green's function (dashed line), and the total vertex part (shaded triangle). (b) Dyson-type equation for the total vertex part, reducing the evaluation of the total vertex part to the problem of electron-electron interaction via exchange of phonons. The shaded square is the total vertex part for this problem.

with $\dot{X}(t)=\exp(iHt/\hbar)\dot{X}\exp(-iHt/\hbar)$. An expression for $\dot{X}$ can easily be obtained from Eq. (13),

$$\dot{X}=-\frac{i}{\hbar}\sum_{\substack{n\ell n'\ell'\\ \mathbf{q}jX}}\lambda^2 q_y M_X^{\mathbf{q}j}\binom{n'\ell'}{n\ell}(b_{-\mathbf{q}j}^{\dagger}+b_{\mathbf{q}j})C_{n'\ell' X-\lambda^2 q_y}^{\dagger}C_{n\ell X}. \tag{16}$$

Introducing the retarded bosonic Green's function

$$\Pi^R(t-t')=-i\vartheta(t-t')\langle[\dot{X}(t)\dot{X}(t')-\dot{X}(t')\dot{X}(t)]\rangle, \tag{17}$$

and noting that

$$\phi_{xx}(t)=\frac{ie^2}{\hbar}\langle[\dot{X}\dot{X}(t)-\dot{X}(t)\dot{X}]\rangle, \tag{18}$$

one can express the dissipative conductivity in the following way:[27]

$$\sigma_{xx}=\frac{ie^2}{\hbar V_{2d}}\left.\frac{\partial\tilde{\Pi}^R(\omega)}{\partial\omega}\right|_{\omega\to 0}, \tag{19}$$

where the Fourier transform of $\Pi^R(t)$ is given by

$$\tilde{\Pi}^R(\omega)=\int_0^{\infty}e^{i\omega t}\Pi^R(t)dt. \tag{20}$$

Equation (19) reduces the calculation of the dissipative conductivity to the evaluation of the two-particle Green's function (17). The latter can be easily performed using the finite-temperature diagrammatic technique,[26] which is based on the Matsubara Green's function, introduced as

$$\Pi(\tau)=-\vartheta(\tau)\langle\dot{X}(\tau)\dot{X}\rangle-\vartheta(-\tau)\langle\dot{X}\dot{X}(\tau)\rangle, \tag{21}$$

where τ is the imaginary time ($-\beta\leqslant\tau\leqslant\beta$), and $\dot{X}(\tau)$ in this formula is defined as

$$\dot{X}(\tau)=e^{\tau(H-\mu N)}\dot{X}e^{-\tau(H-\mu N)}. \tag{22}$$

Performing an S-matrix expansion of the Green's function $\Pi(\tau)$, and expressing each term in terms of nonperturbed electron and phonon Green's functions, one obtains an infinite series of diagrams, the first terms of which are shown in Fig. 2. This series can be summed graphically to give the diagram of Fig. 3(a). The solid bold lines represent the exact electron Green's function $G_X(n\ell;ip_n)$, and the dashed line represents the exact phonon Green's function $D(\mathbf{q}j;i\omega_m)$. The shaded triangle is the total vertex part of the electron-phonon interaction, which we denote by $\mathcal{M}_X^{\mathbf{q}j}\binom{n'\ell'}{n\ell};ip_n,i\omega_n\big)$.

The Fourier transform $\tilde{\Pi}^R(\omega)$ is obtained from the Fourier transform of $\Pi(\tau)$ by the standard analytical continuation to the real axis,[28] i.e., by the substitution $i\omega_n\to\omega+i\delta$. An analytic expression for the Fourier transform of $\Pi(\tau)$ follows from the diagram of Fig. 3(a):

$$\tilde{\Pi}(i\omega_n)=-\frac{\lambda^4}{\hbar^2\beta^2}\sum_{\substack{n\ell n'\ell'\\ \mathbf{q}jX}}\sum_{i\omega_m}\sum_{ip_n}M_X^{\mathbf{q}j}\binom{n'\ell'}{n\ell}\hat{Q}_y^2\mathcal{M}_{X-\lambda^2 q_y}^{-\mathbf{q}j}\binom{n\ell}{n'\ell'};ip_n,i\omega_m\Big)D(\mathbf{q}j;i\omega_m)G_{X-\lambda^2 q_y}(n'\ell';ip_n+i\omega_m-i\omega_n)G_X(n\ell;ip_n), \tag{23}$$

where the operator $\hat{Q}_y$ acts on the total vertex part $\mathcal{M}_X^{\mathbf{q}j}\binom{n'\ell'}{n\ell};ip_n,i\omega_n\big)$, and chooses the component q_y referring to the nonperturbed phonon line of one of the fermionic angles of the total vertex. The Matsubara frequency $i\omega_n$ has to be inserted in the vertex where $\hat{Q}_y$ acts.

In the next section we shall work in a representation

where the electron Green's function is a matrix. It can be obtained by projecting $G_X(n\ell;ip_n)$ onto the single-particle states of the electron.

III. ENERGY SPECTRUM OF ELECTRONS IN THE PRESENCE OF PHONONS

It is well-known that in the general case, taking into account a perturbation has two effects on a electron gas. One is the renormalization of the energy spectrum, and the other is the introduction of a finite lifetime for electrons. We shall focus here on the energy renormalization effects, in a special case when two Landau levels of different subbands of size quantization approach each other at an energy distance comparable to the characteristic phonon energy. Let 1 (2) be a combined label $n\ell$ for the energy level belonging to the lower (upper) size quantization subband, and hence $\mathcal{E}_1$ and $\mathcal{E}_2$ stand for the energies of these levels, respectively.

The renormalized electron energy spectrum can be extracted from the poles of the electron Green's function. By the virtue of circumstances the electron self-energy is diagonal in the Landau level number, and hence, so is the exact electron Green's function. Therefore one can consider the Green's function of each electron level separately. For level 1 in the presence of level 2, the Dyson equation reads

$$G_{11}(ip_n) = G_{11}^{(0)}(ip_n) + G_{11}^{(0)}(ip_n)\Sigma_{11}(ip_n)G_{11}(ip_n), \quad (24)$$

where $G_{11}^{(0)}(ip_n)$ is the Green's function of the nonperturbed electron of level 1, $\Sigma_{11}(ip_n)$ is the self-energy of the electron of level 1, and ip_n is the imaginary fermionic frequency, with $p_n=(2n+1)\pi/\beta$. The influence of level 2 is manifested indirectly through the self-energy $\Sigma_{11}(ip_n)$. The lowest-order approximation for $\Sigma_{11}(ip_n)$ is given by the diagram in Fig. 4. An analytical expression for this diagram is

$$\Sigma_{11}^{(0)}(ip_n) = \Sigma_{11}^{self}(ip_n) + \Sigma_{11}^{inter}(ip_n), \quad (25)$$

with

$$\Sigma_{11}^{self}(ip_n) = \sum_{\mathbf{q}j} \left| M_X^{\mathbf{q}j}\begin{pmatrix}1\\1\end{pmatrix}\right|^2 \left(\frac{N_\mathbf{q}+n_F(\xi_1)}{ip_n+\omega_{\mathbf{q}j}-\xi_1} + \frac{N_\mathbf{q}+1-n_F(\xi_1)}{ip_n-\omega_{\mathbf{q}j}-\xi_1}\right), \quad (26)$$

and

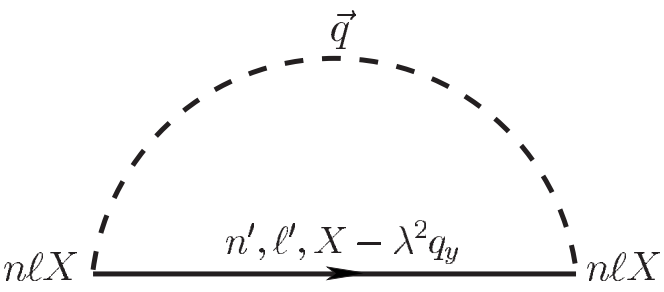

FIG. 4. The first term of the pertubration expansion of the electron self-energy.

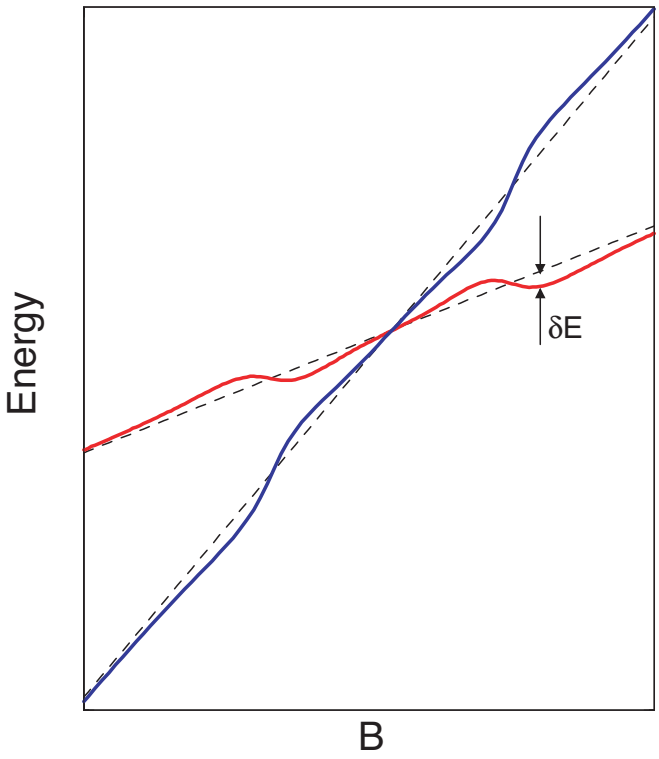

FIG. 5. (Color online) Qualitative behavior of the Landau levels in the vicinity of a level-crossing. The dashed lines represent the nonperturbed Landau levels.

$$\Sigma_{11}^{inter}(ip_n) = \sum_{\mathbf{q}j} \left| M_X^{\mathbf{q}j}\begin{pmatrix}2\\1\end{pmatrix}\right|^2 \left(\frac{N_\mathbf{q}+n_F(\xi_2)}{ip_n+\omega_{\mathbf{q}j}-\xi_2} + \frac{N_\mathbf{q}+1-n_F(\xi_2)}{ip_n-\omega_{\mathbf{q}j}-\xi_2}\right), \quad (27)$$

where $\xi_i=\mathcal{E}_i-\mu$. The self-energy part Σ_{11}^{self} accounts for the renormalization of the energy level in the absence of other levels. This renormalization is not expected to change significantly in the neighborhood of the level crossing, and we shall not take it into account, considering that it has been included initially in the electron effective mass. This assumption is correct as long as the deviation from the nonperturbated energy levels is small in comparison with the characteristic phonon energy.

The real part of the retarded self-energy can be used to find the renormalized electron energy, which is equivalent to using Brillouin-Wigner perturbation theory.[26] The renormalized energy can be oftained from the following equation:

$$E - \mathcal{E}_1 - \mathrm{Re}\,\Sigma_{11}^{inter}(E) = 0. \quad (28)$$

Solving Eq. (28) with respect to E, one finds the renormalized electron energy level $\tilde{\mathcal{E}}_1$. A similar equation holds for level 2.

Figure 5 shows the qualitative dependence of the renormalized energy levels $\tilde{\mathcal{E}}_1$ and $\tilde{\mathcal{E}}_2$ on the magnetic field B for the crossing of Landau levels $\ell=1$ and $\ell=0$ of the first and second subbands of size quantization, respectively. One can

see that there are two values of B on both sides of the crossing, where repulsion of levels changes to attraction. We can prove analytically that this happens when the energy distance betwen the two unperturbed electron levels is close to the characteristic phonon energy $\hbar s/\lambda_+$, where λ_+ is λ at the level crossing. This characteristic energy of phonons will reappear in Sec. IV in the calculation of the dissipative conductivity σ_{xx}, where peculiar behavior of σ_{xx} is found at the same characteristic magnetic fields on both sides of the level crossing.

Notably, the typical value of the deviation δE of the renormalized levels from the unperturbed ones is very small for all temperatures of interest in GaAs systems. A rough analytical estimate gives $\delta E \sim \alpha T$ at temperatures $T \gg \hbar s/\lambda_+$, but still low enough for the perturbation theory to work, $T \ll \hbar s/(\alpha\lambda_+)$. The dimensionless coupling constant of electron-phonon interaction $\alpha \simeq 0.1[(100\ \text{Å})/\lambda]^2$ for GaAs.[29] Thus for $B=6.6$ T and $T=10$ K one obtains $\delta E \sim 10^{-1}$ meV. Numerical calculations give an even smaller value of $\delta E \sim 10^{-3}$ meV. We shall neglect these energy corrections in our further calculations, stating only that the electron levels intersect in the presence of equilibrium phonons.

IV. DISSIPATIVE CONDUCTIVITY

The dissipative conductivity σ_{xx} is calculated using Eq. (19) and the expression for the Fourier transform of the two-particle correlation function (23). The results of the perturbation theory are obtained using the S-matrix expansion for the electron Green's functions. The effects of renormalization of the phonon spectrum due to the presence of electrons will not be taken into account in what follows. We have made a rougher approximation already, neglecting the interface phonon modes and the variance of the sound velocity, as one goes from the quantum well to the substrate material. We use the Green's function of nonperturbed phonons instead of the exact phonon Green's function.

A. The one-phonon process

This process is described by the first diagram in Fig. 2. The analytical expression of this diagram reads

$$\tilde{\Pi}_0(i\omega_n) = -\frac{e^2}{\hbar^2}\lambda^4 \frac{1}{\beta}\sum_{i\omega_m}\frac{1}{\beta}\sum_{ip_n}\sum_{\substack{n\ell n'\ell' \\ \mathbf{q}jX}} q_y^2 \left| M_X^{\mathbf{q}j}\begin{pmatrix} n'\ell' \\ n\ell \end{pmatrix}\right|^2 \times D^{(0)}(\mathbf{q}j; i\omega_m) G^{(0)}_{X-\lambda^2 q_y}(n'\ell'; ip_n + i\omega_m - i\omega_n) \times G_X^{(0)}(n\ell; ip_n), \tag{29}$$

where $G_X^{(0)}(n\ell, ip_n) = 1/(ip_n - \xi_{n\ell})$ is the unperturbed electron Green's function, and $D^{(0)}(\mathbf{q}j, i\omega_m) = -2\hbar\omega_{\mathbf{q}j}/(\omega_m^2 + \hbar^2\omega_{\mathbf{q}j}^2)$ is the unperturbed phonon Green's function. The summation over the discrete Matsubara frequencies in Eq. (29) can be performed easily, and using Eq. (19), one arrives at the following expression for the dissipative conductivity:

$$\sigma_{xx} = \frac{1}{V_{2d}}\frac{e^2}{\hbar^2}\lambda^4\pi\beta \sum_{\substack{n\ell n'\ell' \\ \mathbf{q}jX}} q_y^2 \left| M_X^{\mathbf{q}j}\begin{pmatrix} n'\ell' \\ n\ell \end{pmatrix}\right|^2 f(\xi_{n\ell})\{N_{\mathbf{q}j}[1 - f(\xi_{n\ell} + \hbar\omega_{\mathbf{q}j})]\delta(\xi_{n'\ell'} - \xi_{n\ell} - \hbar\omega_{\mathbf{q}j}) + (N_{\mathbf{q}j} + 1)[1 - f(\xi_{n\ell} - \hbar\omega_{\mathbf{q}j})]\delta(\xi_{n'\ell'} - \xi_{n\ell} + \hbar\omega_{\mathbf{q}j})\}, \tag{30}$$

where $f(\xi) = [\exp(\beta\xi) + 1]^{-1}$ is the fermionic distribution function and $N_{\mathbf{q}j} = [\exp(\beta\hbar\omega_{\mathbf{q}j}) - 1]^{-1}$ is the bosonic distribution function.

Equation (30) has the following physical interpretation. The electron can be scattered from the lower (upper) Landau level to the other one by absorbing (emitting) a phonon. Each of these processes leads to the diffusion of the electron within these two Landau levels. Thus one can think of the diffusion of the electron in the upper level induced by the emission of a phonon, and of the diffusion of the electron in the lower level induced by the absorption of a phonon. At thermal equlibrium the number of electrons transferred up and down is equal, which can be expressed mathematically by the identity

$$f(\mathcal{E}_1)[1 - f(\mathcal{E}_2)]N_{q_0} = f(\mathcal{E}_2)[1 - f(\mathcal{E}_1)](N_{q_0} + 1), \tag{31}$$

where $q_0 = |\mathcal{E}_2 - \mathcal{E}_1|/(\hbar s)$. Threfore it is not important that at each scattering event the electron is transferred from one Landau level to the other. In a diffusive motion the "memory" after one scattering event is lost. Thus one can safely assign to each Landau level a diffusion coefficient, and disregard the conservation of the number of electrons during an inelastic process. This way we interpret formula (30) as a generalized Einstein relation,

$$\sigma_{xx} = \frac{e^2}{2\pi\lambda^2}\frac{f(\mathcal{E}_1)}{T}D_{xx}^{1\to 2} + \frac{e^2}{2\pi\lambda^2}\frac{f(\mathcal{E}_2)}{T}D_{xx}^{2\to 1}, \tag{32}$$

with the diffusion coefficients being calculated according to the formula

$$D_{xx}^{\alpha\to\beta} = \frac{1}{2}\sum_{\mathbf{q}j}\sum_{X'}(X - X')^2 W_{XX'}^{\alpha\to\beta}. \tag{33}$$

The probability $W_{XX'}^{\alpha\to\beta}$ for an electron in level α to be scattered from point X to point X', and at the same time to be transferred to level β, can as well be calculated using the Fermi golden rule, which straightforwardly yields

$$W_{XX'}^{1\to 2} = \frac{2\pi}{\hbar}\left| M_X^{\mathbf{q}j}\begin{pmatrix} 2 \\ 1 \end{pmatrix}\right|^2 [1 - f(\mathcal{E}_2)]N_{\mathbf{q}j}\delta_{X',X-\lambda^2 q_y} \times \delta(\mathcal{E}_2 - \mathcal{E}_1 - \hbar\omega_{\mathbf{q}j}),$$

$$W_{XX'}^{2\to 1} = \frac{2\pi}{\hbar}\left| M_X^{-\mathbf{q}j}\begin{pmatrix} 1 \\ 2 \end{pmatrix}\right|^2 [1 - f(\mathcal{E}_1)](N_{-\mathbf{q}j} + 1)\delta_{X',X-\lambda^2 q_y} \times \delta(\mathcal{E}_2 - \mathcal{E}_1 + \hbar\omega_{-\mathbf{q}j}). \tag{34}$$

The processes of phonon absorption and emission give equal contributions into σ_{xx}. Equation (32) together with Eqs. (31) and (33) give exactly the same result for σ_{xx} as Eq. (30) when the contribution from the levels other than the two

considered ones is neglected in Eq. (30). Finally, we note that such a simple picture of independent diffusion of electrons in each Landau level is not generally valid in a nonequilibrium situation.

Taking into account the contributions from the deformation potential (*dp*), longitudinal-phonon piezoelectric (*peLA*), and transverse-phonon piezoelectric (*peTA*) mechanisms of electron-phonon interaction, one obtains

$$\sigma_{xx} = \sigma_{xx}^{dp} + \sigma_{xx}^{peLA} + \sigma_{xx}^{peTA}, \tag{35}$$

where

$$\sigma_{xx}^{dp} = \frac{\sqrt{2}\ell'!}{\pi^2\ell!}\frac{e^2}{\hbar}\frac{\Xi_{q_{0LA}}^2\hbar}{2\rho_c s_{LA}\lambda^4}\frac{1}{T_\lambda T}f(\xi_1)[1 - f(\xi_2)]N_{q_{0LA}}\left(\frac{q_{0LA}\lambda}{\sqrt{2}}\right)^{5+2(\ell-\ell')}\int_0^1 dx Z(q_{0LA}x)(1-x^2)^{\ell-\ell'+1}[L_{\ell'}^{\ell-\ell'}[(1-x^2)q_{0LA}^2\lambda^2/2]]^2 e^{-(1-x^2)q_{0LA}^2\lambda^2/2}, \tag{36}$$

and

$$\sigma_{xx}^{peLA} = \frac{9\ell'!}{8\sqrt{2}\pi^2\ell!}\frac{e^2}{\hbar}\frac{e^2\hbar\beta_{q_{0LA}}^2}{2\rho_c s_{LA}\lambda^2}\frac{1}{T_\lambda T}f(\xi_1)[1 - f(\xi_2)]N_{q_{0LA}}\left(\frac{q_{0LA}\lambda}{\sqrt{2}}\right)^{3+2(\ell-\ell')}\int_0^1 dx Z(q_{0LA}x)x^2(1-x^2)^{\ell-\ell'+3}[L_{\ell'}^{\ell-\ell'}[(1-x^2)q_{0LA}^2\lambda^2/2]]^2 e^{-(1-x^2)q_{0LA}^2\lambda^2/2}, \tag{37}$$

and

$$\sigma_{xx}^{peTA} = \frac{\ell'!}{8\sqrt{2}\pi^2\ell!}\frac{e^2}{\hbar}\frac{e^2\hbar\beta_{q_{0TA}}^2}{2\rho_c s_{TA}\lambda^2}\frac{1}{T_\lambda T}f(\xi_1)[1 - f(\xi_2)]N_{q_{0TA}}\left(\frac{q_{0TA}\lambda}{\sqrt{2}}\right)^{3+2(\ell-\ell')}\int_0^1 dx Z(q_{0TA}x)(9x^4 - 2x^2 + 1)(1-x^2)^{\ell-\ell'+2}[L_{\ell'}^{\ell-\ell'}[(1-x^2)q_{0TA}^2\lambda^2/2]]^2 e^{-(1-x^2)q_{0TA}^2\lambda^2/2}. \tag{38}$$

Here, $q_{0j}=(\mathcal{E}_2-\mathcal{E}_1)/\hbar s_j$, and the form factor $Z(q_z)=|F_{n_1n_2}(q_z)|^2$ depends on the form of the quantum well potential $V(z)$.

The largest value of σ_{xx} is obtained for the crossing of the Landau levels with the smallest possible numbers, i.e., $\ell=1$ and $\ell'=0$, and belonging to the two lowest subbands of size quantization. For the case of a parabolic quantum well of characteristic size a ($E_{12}=\hbar^2/ma^2$), the calculations can be performed analytically, using $Z(q_z)=(q_z^2a^2/2)\times\exp(-q_z^2a^2/2)$, and the result for $ms^2 \ll E_{12}$ reads

$$\sigma_{xx}^{dp} = \frac{e^2}{h}C_1\alpha_{dp}\frac{T_\lambda}{T}f(\xi_1)[1 - f(\xi_2)]N_{q_{0LA}}\lambda^7a^2q_{0LA}^9 \times\exp\left(-\frac{\lambda^2q_{0LA}^2}{2}\right), \tag{39}$$

$$\sigma_{xx}^{peLA} = \frac{e^2}{h}C_2\alpha_{peLA}\frac{T_\lambda}{T}f(\xi_1)[1 - f(\xi_2)]N_{q_{0LA}}\lambda^5a^2q_{0LA}^7 \times\exp\left(-\frac{\lambda^2q_{0LA}^2}{2}\right), \tag{40}$$

$$\sigma_{xx}^{peTA} = \frac{e^2}{h}C_3\alpha_{peTA}\frac{T_\lambda}{T}f(\xi_1)[1 - f(\xi_2)]N_{q_{0TA}}\lambda^5a^2q_{0TA}^7 \times\exp\left(-\frac{\lambda^2q_{0TA}^2}{2}\right), \tag{41}$$

where C_1, C_2, and C_3 are weak functions of the magnetic field in the neighborhood of crossing. At the crossing point ($\lambda=a$), we obtain $C_1=1/105\pi$, $C_2=6/5005\pi$, and $C_3=10/9009\pi$. The effective coupling constants of electron-phonon interaction for different mechanisms were introduced in the following way:

$$\alpha \equiv \alpha_{dp} = \frac{\hbar\Xi_0^2}{2\rho_c s_{LA}\lambda^4}\frac{1}{T_\lambda^2}, \tag{42}$$

$$\alpha_{peLA} = \frac{e^2\beta_0^2}{2\rho_c s_{LA}^3\hbar}, \tag{43}$$

$$\alpha_{peTA} = \frac{e^2\beta_0^2}{2\rho_c s_{TA}^3\hbar}. \tag{44}$$

Figure 6 shows the dependence of σ_{xx} [Eq. (35)] on the magnetic field B in the vicinity of an intersection of two Landau levels in a parabolic quantum well. The magnetic field corresponding to the intersection of the levels is that of the minimum on the graph. The two maxima appear at magnetic fields close to those at which the electron-phonon scattering rate is maximal. The distance between the Landau levels at the maxima of σ_{xx} is of the order of $T_\lambda=\hbar s/\lambda$. In computing the dependence of σ_{xx} on the magnetic field, the electron concentration n_{2D} was kept constant and the chemical potential μ was calculated according to the following formula:

$$\mu = \frac{\mathcal{E}_1+\mathcal{E}_2}{2} - T\ln\left(\frac{\sqrt{1+\zeta^2\sinh^2\frac{\mathcal{E}_2-\mathcal{E}_1}{2T}} - \zeta\cosh\frac{\mathcal{E}_2-\mathcal{E}_1}{2T}}{1+\zeta}\right), \tag{45}$$

with

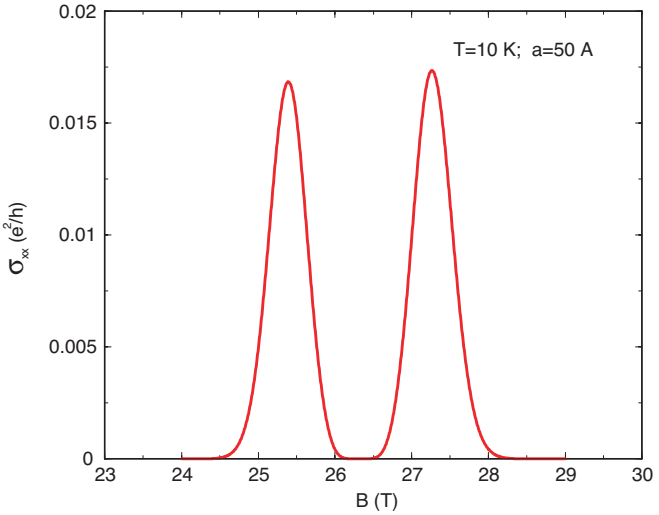

FIG. 6. (Color online) The dissipative conductivity as a function of magnetic field in the vicinity of the crossing of Landau levels $\ell=1$ and $\ell=0$, belonging to the first and second size-quantization subbands, respectively. Material parameters are taken as for a GaAs system.

$$\zeta = \frac{\lambda^2}{\lambda_+^2}\nu_0 - (N_0 + 1), \tag{46}$$

where ν_0 is the filling factor at $\lambda=\lambda_+$, and N_0 is the number of Landau levels below the two considered ones. The electron concentration n_{2D} is related to the filling factor ν_0 in the usual way, $n_{2D}=\nu_0/2\pi\lambda_+^2$.

We compare different contributions to σ_{xx} [see Eq. (35)] in Fig. 7. At a small value of the quantum well width a, the deformation potential mechanism (dashed line) dominates the dissipative conductivity [Fig. 7(a)]. However, at a larger value of a, the piezoelectric mechanism is the dominant contribution to σ_{xx}, e.g., the piezoelectric interaction with the transverse phonon mode (solid line) in Fig. 7(b). This is not surprising, since the deformation potential mechanism contains one extra power of the phonon momentum, as is seen from the matrix element (4). The relevant phonon momentum is related to the quantum well width and to the magnetic length, $q^{-1}\sim a\sim\lambda$. The characteristic well width at which the crossover from the deformation potential to the piezoelectric mechanism happens is given by $a\sim\Xi_0\kappa/eh_{14}$. We find that although this criterion gives a characteristic $a\sim 700$ Å, the actual crossover happens at a smaller value of a [see Fig. 7(b)], owing to a larger overlap integral of the electron with the phonons via the piezoelectric interaction.

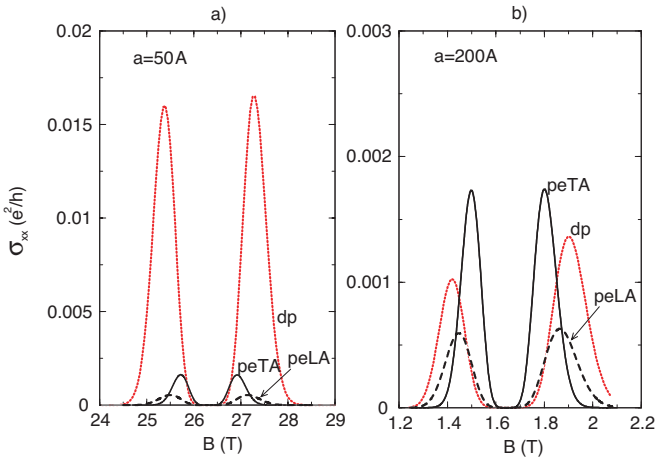

FIG. 7. (Color online) A comparison of contributions to σ_{xx} from different mechanisms of electron-phonon interaction at two values of the quantum well width a. The lines are labeled as follows: the deformation potential mechanism–*dp*, the piezoelectric longitudinal mechanism–*peLA*, and the piezoelectric transversal mechanism–*peTA*.

As it has already been mentioned in the introduction to our paper, the main contribution to the conductivity in experimentally available systems comes from impurities. However, it can be clearly seen from the plot in Fig. 6 that the phonon-induced conductivity is not negligibly small comparing to a typical value of impurity-induced conductivity, which is of the order of the conductance quantum for a partially filled Landau level. The disorder-mediated magnetoconductivity is noticeably smaller in wide parabolic quantum wells,[30] which represent the best system for observation of the discussed effect. Modern experimental techniques should be able to separate the two mechanisms, especially since the phonon-induced contribution to the conductivity has a distinguished two-peak structure and completely different magnetic field and temperature dependencies. In addition, in our calculations we use parameters of GaAs, which is known to have very weak electron-phonon coupling. For some other materials this effect can be much stronger. The enhancement of electron-phonon scattering near the Landau level intersection described in our work is possibly responsible for some features observed in magnetothermal conductivity of highly oriented pyrolitic graphite.[31,32] In the presence of nonequilibrium phonons[4–7] the electron-phonon scattering mechanism might become dominant.

B. The two-phonon process

When the distance between the two Landau levels on both sides of the Fermi level is much greater than $\hbar s/\lambda$, the one-phonon electron transitions become inefficient, and the two-phonon ones should be taken into account. The two-phonon process associated with the electron transition between two Landau levels was considered in Ref. 8. It was shown in Ref. 33 that the two-phonon scattering is responsible for dissociation of magnetorotons in the phonon absorption spectroscopy experiments[6] in the fractional quantum Hall regime. The two-phonon process associated with the scattering of the electron within the same infinitely narrow Landau level was considered in Ref. 20. Since there was a mistake in Ref. 20, we reconsider the latter process here again.

Consider one Landau level only, which has a δ-function density of states. Within this infinitely narrow energy level, one-phonon electron transitions are not possible, since phonons with zero energy are not efficient for electron scattering, and, moreover, there are no such phonons because the phonon density of states is proportional to $\omega_{\mathbf{q}j}^2$. However,

multiple-phonon scattering makes it possible to transfer momentum without transferring any energy to the electron. In the simplest case a simultaneous absorption of one phonon with momentum $\mathbf{q}$ and emission of another phonon with momentun $\mathbf{q}'$ transfers a momentum $\mathbf{q}-\mathbf{q}'$ to the electron, and does not change its energy, provided $|\mathbf{q}|=|\mathbf{q}'|$.

All two-phonon processes are described by the diagrams (b)–(e) of Fig. 2. The main contribution is given by processes which do not involve the transition of the electron to another Landau level. The diagram (b) accounts for the renormalization of the phonon spectrum and will not be taken into account in this paper. The dissipative conductivity σ_{xx} can be presented in the following form:

$$\sigma_{xx}=\frac{e^2}{2\pi\lambda^2}f(\xi)[1-f(\xi)]\frac{D}{T}. \tag{47}$$

The diffusion coefficient for the deformation potential type of interaction is

$$D^{dp}=\frac{\Xi_0^4\lambda^4}{2\rho_c^2 s_{LA}^5\hbar^2}\frac{1}{(2\pi)^5}\int d^3q\int d^3q'(q_y-q_y')^2N_q(1+N_{q'})\times\delta(q-q')[L_\ell(\lambda^2q_\perp^2/2)L_\ell(\lambda^2q_\perp'^2/2)]^2|\times Z(q_z)Z(-q_z')|^2e^{-\lambda^2(q_\perp^2+q_\perp'^2)/2}\sin^2\{\lambda^2\mathbf{e}_z[\mathbf{q}_\perp\times\mathbf{q}_\perp']/2\}, \tag{48}$$

where $\mathbf{e}_z$ is the unit vector normal to the quantum well plane.

At $T\ll T_\lambda$ the diffusion coefficient for the lowest Landau level ($l=0$) is given by

$$D=A_1\alpha^2\lambda s\left(\frac{T}{T_\lambda}\right)^{11}, \tag{49}$$

where $A_1=2^9\pi^7/297\approx 5.2\times 10^3$.

At $\hbar\omega_c\gg T\gg T_\lambda$ the diffusion coefficient for the same Landau level is given by

$$D=A_2\alpha^2\lambda s\left(\frac{T}{T_\lambda}\right)^2, \tag{50}$$

in which

$$A_2=\frac{3}{2^{9/2}\pi^{5/2}}\int_0^1\frac{dx}{(1+x)^{3/2}}\{1-F[5/4,7/4;1;-4x/(1+x)^2]\}K(\sqrt{x}), \tag{51}$$

where $K(z)$ is an elliptic integral and $F(\alpha,\beta;n;z)$ is a hypergeometric function. The numerical value of the constant A_2 is approximately 5.7×10^{-3}.

V. LEVEL-BROADENING BY PHONONS

The effects of multiphonon scattering are important at high temperatures. We can solve the Dyson equation analytically for two Landau levels in the so-called damping theoretical approximation.[2,25] In this approximation the total vertex [Fig. 3(b)] is calculated to first order, whereas the Dyson equation is solved in a self-consistent way. It can be justified for temperatures or level broadening much larger than the characteristic phonon energy, and for spectral regions away from the spectral edges. We first recall the results for a single Landau level[2] and then consider the intersection of two Landau levels.

For a single Landau level, it is required that (i) transitions to higher Landau levels can be neglected ($\hbar\omega_c\gg T$), and (ii) the scattering with phonons is almost elastic, i.e., $\hbar s/\lambda\ll T,\Gamma$. The self-energy can then be written in the following form:

$$\Sigma_\ell(E)=\frac{1}{4}\Gamma_\ell^2 G_\ell(E), \tag{52}$$

where

$$\Gamma_\ell^2=8\sum_{\mathbf{q}j}N_{\mathbf{q}j}\left|M_X^{\mathbf{q}j}\begin{pmatrix}\ell\\ \ell\end{pmatrix}\right|^2,$$

which gives an expression for the electron Green's function:

$$G_\ell^{\pm}(E)=\frac{2}{E-\mathcal{E}_\ell\pm\sqrt{(E-\mathcal{E}_\ell)^2-\Gamma_\ell^2}}. \tag{53}$$

The sign in Eq. (53) is chosen so as to restore the distant energy asymptote, $G_\ell(E)\propto 1/(E-\mathcal{E})$. The spectral density of states $A_\ell=-2\,\mathrm{Im}[G_\ell^R(E)]$ is given by

$$A_\ell(E)=i[G_\ell^+(E)-G_\ell^-(E)]=\frac{4}{\Gamma_\ell}\sqrt{1-\frac{(E-\mathcal{E}_\ell)^2}{\Gamma_\ell^2}}, \tag{54}$$

$$|E-\mathcal{E}_\ell|<\Gamma_\ell,$$

and $A_\ell(E)=0$ elsewhere. In this approximation, no renormalization of the electron energy occurs.

For two intersecting Landau levels we require that (i) transitions from either of the two Landau levels to other Landau levels can be neglected, and (ii) the broadening of each of the two considered Landau levels is larger than the characteristic phonon energy T_λ. For the self-energy we obtain

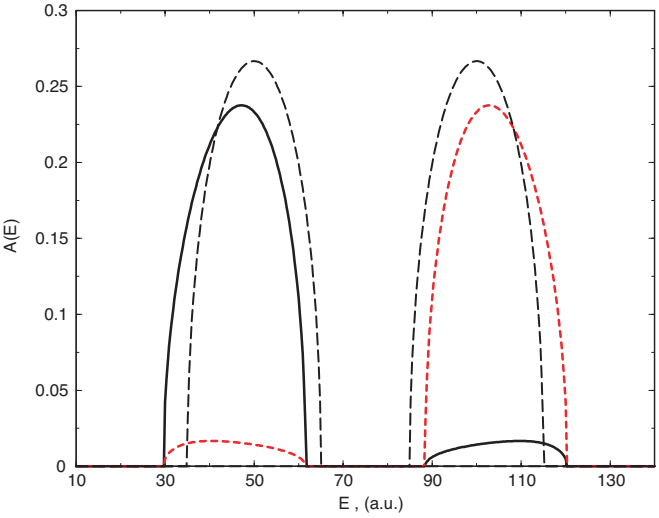

FIG. 8. (Color online) Level mixing.

$$\Sigma_\alpha(E) = \frac{1}{4}\sum_\beta \Gamma^2_{\alpha\beta} G_\beta(E), \tag{55}$$

in which

$$\Gamma^2_{\alpha\beta} = 8\sum_{\mathbf{q}j} N_{\mathbf{q}j} \left| M_X^{\mathbf{q}j}\begin{pmatrix}\beta\\ \alpha\end{pmatrix}\right|^2,$$

where $\alpha=1,2$ numbers the two considered Landau levels. Using the identity $\Sigma_\alpha(E)=E-\mathcal{E}_\alpha-1/G_\alpha(E)$, we obtain from Eq. (55) the following set of coupled equations:

$$(E-\mathcal{E}_1)G_1 - \frac{1}{4}(\Gamma^2_{11}G_1 + \Gamma^2_{12}G_2)G_1 = 1,$$

$$(E-\mathcal{E}_2)G_2 - \frac{1}{4}(\Gamma^2_{22}G_2 + \Gamma^2_{12}G_1)G_2 = 1, \tag{56}$$

which determine the Green's functions of the two Landau levels. If we consider the energy region $\mathcal{E}_1<E<\mathcal{E}_1$ on one side of the crossing, the solution of Eqs. (56) reads

$$G_1(E) = G_1^-(E)\left(1 - \frac{\Gamma^2_{12}G_2^+(E)}{4\sqrt{(E-\mathcal{E}_1)^2-\Gamma_1^2}}\right)^{-1}, \tag{57}$$

$$G_2(E) = G_2^+(E)\left(1 + \frac{\Gamma^2_{12}G_1^-(E)}{4\sqrt{(E-\mathcal{E}_2)^2-\Gamma_2^2}}\right)^{-1}, \tag{58}$$

where $G_\alpha^\pm(E)$ are given by Eq. (53).

The resulting spectral density of states is plotted in Fig. 8.

VI. CONCLUSIONS

In this paper we considered the scattering of electrons by equilibrium phonons in a two-subband quasi-two-dimensional electron gas in a quantizing magnetic field. A resonant enhancement of the dissipative conductivity was found in the vicinity of an intersection of two Landau levels, belonging to different size-quantization subbands.

ACKNOWLEDGMENTS

We are grateful to V. I. Perel and V. Karpus for stimulating discussions and to D. G. W. Parfitt for valuable advice. M.E.P. acknowledges the hospitality of the ICCMP's staff and the financial support received from MCT and FINEP (Brazil).

*Present address: Department of Physics and Astronomy, University of Basel, Klingelbergstrasse 82, CH-4056 Basel, Switzerland. Electronic address: vitaly.golovach@unibas.ch
†Electronic address: m.e.portnoi@exeter.ac.uk

[1] M. S. Erukhimov, Fiz. Tekh. Poluprovodn. (S.-Peterburg) **3**, 194 (1969) [Sov. Phys. Semicond. **3**, 162 (1969)].
[2] V. V. Korneev, Fiz. Tverd. Tela (Leningrad) **19**, 357 (1977) [Sov. Phys. Solid State **19**, 205 (1977)].
[3] K. A. Benedict, R. K. Hills, and C. J. Mellor, Phys. Rev. B **60**, 10 984 (1999).
[4] K. A. Benedict, J. Phys.: Condens. Matter **3**, 1279 (1991).
[5] G. A. Toombs, F. W. Sheard, D. Neilson, and L. J. Challis, Solid State Commun. **64**, 577 (1987).
[6] U. Zeitler, A. M. Devitt, J. E. Digby, C. J. Mellor, A. J. Kent, K. A. Benedict, and T. Cheng, Phys. Rev. Lett. **82**, 5333 (1999).
[7] *Electron-Phonon Interactions in Low-Dimensional Structures*, edited by L. J. Challis (Oxford University Press, Oxford, 2003).
[8] V. I. Fal'ko and L. J. Challis, J. Phys.: Condens. Matter **5**, 3945 (1993).
[9] P. A. Maksym, in *High Magnetic Fields in Semiconductor Physics III*, edited by G. Landwehr (Springer-Verlag, Berlin, 1992), p. 254.
[10] V. M. Apalkov and M. E. Portnoi, Physica E (Amsterdam) **15**, 202 (2002).
[11] V. M. Apalkov and M. E. Portnoi, Phys. Rev. B **65**, 125310 (2002).
[12] I. M. Lifshitz, Zh. Eksp. Teor. Fiz. **33**, 1569 (1960) [Sov. Phys. JETP **11**, 1130 (1969)].
[13] N. N. Ablyazov, M. Yu. Kuchiev, and M. E. Raikh, Phys. Rev. B **44**, 8802 (1991).
[14] D. V. Lang, in *Deep Centers in Semiconductors*, edited by S. T. Pantelides (Gordon and Breach, New York, 1986), p. 486.
[15] A. Kastalsky and J. C. M. Hwang, Solid State Commun. **51**, 317 (1984).
[16] I. V. Kukushkin, K. von Klitzing, K. Ploog, V. E. Kirpichev, and B. N. Shepel, Phys. Rev. B **40**, 4179 (1989).
[17] A. J. Turberfield, S. R. Haynes, P. A. Wright, R. A. Ford, R. G. Clark, J. F. Ryan, J. J. Harris, and C. T. Foxon, Phys. Rev. Lett. **65**, 637 (1990).
[18] A. S. Plaut, K. von Klitzing, I. V. Kukushkin, and K. Ploog, in *Proceedings of the 20th International Conference on the Physics of Semiconductors*, edited by E. M. Anastassakis and J. D. Joannopoulos (World Scientific, London, 1990), Vol. 2, p. 1529.
[19] I. V. Kukushkin, V. B. Timofeev, K. von Klitzing, and K. Ploog, *Festkörperprobleme (Advances in Solid State Physics)*, edited by U. Rössler (Vieweg, Braunschweig, 1988), Vol. 28, p. 21.
[20] Yu. A. Bychkov, S. V. Iordanski, and G. M. Eliashberg, Pis'ma Zh. Eksp. Teor. Fiz. **34**, 496 (1981) [JETP Lett. **34**, 473 (1981)].
[21] J. P. Wolfe and M. R. Hauser, Ann. Phys. **4**, 99 (1995).
[22] R. Kubo, J. Phys. Soc. Jpn. **12**, 570 (1957).
[23] L. D. Landau and E. M. Lifshitz, *Quantum Mechanics (Non-Relativistic Theory)* (Pergamon Press, Oxford, 1977).
[24] R. Kubo, H. Hasegawa, and N. Hashitsume, J. Phys. Soc. Jpn. **14**, 56 (1959).
[25] R. Kubo, S. Miyake, and N. Hashitsume, *Solid State Physics*, edited by F. Seitz and D. Turnbull (Academic Press, New York, 1965), Vol. 17, p. 169.
[26] See, e.g., G. D. Mahan, *Many-Particle Physics* (Plenum Press, New York, 1981).
[27] A. Asihara, *Statistical Physics* (Academic Press, New York, 1971); K. Efetov, *Supersymmetry in Disorder and Chaos*

(Cambridge University Press, Cambridge, 1997).
[28] A. A. Abrikosov, L. P. Gor'kov, and Dzyaloshinskii, *Methods of Quantum Field Theory in Statistical Physics* (Pergamon Press, Oxford, 1965).
[29] Note that $\alpha \sim B$. For more information see V. F. Gantmakher and Y. B. Levinson, *Carrier Scattering in Metals and Semiconductors* (North-Holland, Amsterdam, 1987).
[30] G. M. Gusev, A. A. Quivy, T. E. Lamas, J. R. Leite, O. Estibals, and J. C. Portal, Phys. Rev. B **67**, 155313 (2003).
[31] R. Ocaña, P. Esquinazi, H. Kempa, J. H. S. Torres, and Y. Kopelevich, Phys. Rev. B **68**, 165408 (2003).
[32] K. Ulrich and P. Esquinazi, J. Low Temp. Phys. **137**, 217 (2004).
[33] V. M. Apalkov and M. E. Portnoi, Phys. Rev. B **66**, 121303(R) (2002).